Article

The Influence of Carbonate Binder Content on the Mechanical and Physical Properties of Artificial Lightweight Aggregates Produced by Carbonization Using Wood Waste Fly Ash

Vitoldas Vidikas * and Algirdas Augonis

Faculty of Civil Engineering and Architecture, Kaunas University of Technology, Studentu St. 48, LT-51367 Kaunas, Lithuania; algirdas.augonis@ktu.lt
* Correspondence: vitoldas.vidikas@ktu.edu; Tel.: +370-67865186

Abstract

Large amounts of wood waste fly ash (WWFA) are generated in bioenergy plants, yet their potential for reuse in construction materials remains underexplored. In this study, artificial lightweight aggregates (ALWAs) were produced by cold-bonded granulation of WWFA with hydrated lime, followed by carbonation curing (20 °C, 64% RH, 19% CO_2). The aggregates were evaluated according to EN 13055:2016 classification criteria, with testing performed following the relevant European standards, including EN 1097-3 and EN 1097-6 for density and water absorption, EN 1097-11 for crushing resistance, and EN 1367-7 for freeze–thaw resistance. All ALWAs met the lightweight aggregate classification, with bulk densities of 1010.9–1060.0 kg/m^3 and crushing resistances up to 2.74 N/mm^2, exceeding that of lightweight expanded clay aggregate (LECA) (1.26 N/mm^2). XRD confirmed $CaCO_3$ formation, SEM revealed binder- and w/m-dependent porosity and crystal morphology, and freeze–thaw resistance indicated suitability for non-structural applications. These results demonstrate that WWFA-based ALWAs are a sustainable alternative to natural aggregates, combining waste valorization with competitive performance.

Keywords: artificial lightweight aggregate; wood waste fly ash; granulation; carbonization; CO_2

1. Introduction

During the combustion of biomass, particularly wood waste, two primary types of ash are produced: wood waste fly ash (WWFA), which rises with flue gases, and wood waste bottom ash, which accumulates at the base of the combustion chamber [1]. WWFA consists of fine, powdery particles that become airborne with flue gases and are subsequently captured by filters; due to its high surface area and reactive mineral content, including CaO, SiO_2, and K_2O, it exhibits significant pozzolanic activity, making it suitable as a binder in cementitious materials and artificial aggregates [2]. In contrast, bottom ash comprises coarser, heavier fragments deposited at the base of the combustion chamber, with lower reactivity, and is often used as an inert filler or coarse aggregate [3]. The relative proportions of WWFA and bottom ash vary depending on the combustion technology and operating conditions, with bottom ash frequently accounting for the majority of the ash generated. The distinction between these ash types is critical, as the fine, reactive nature of WWFA makes it more effective in supporting microstructural development and strength in lightweight aggregates produced via cold-bonded granulation and carbonation curing [4].

In Lithuania, wood combustion processes generate approximately 19,800 tons of ash waste annually. Despite this considerable volume, only a limited fraction is currently utilized within the construction sector or for other beneficial applications. One promising avenue for recycling this by-product is its use in the production of ALWAs. These aggregates can be manufactured using various techniques, such as cold bonding, autoclaving, or sintering [5]. Wood combustion primarily produces inorganic ash waste, which is often either recovered for low-value uses or sent to landfills, with minimal amounts being recycled [6]. However, rising energy demands continue to increase ash generation each year, while the availability of designated ash disposal sites remains limited. Therefore, reusing WWFA, either as a supplementary material in concrete or as a raw material in the fabrication of ALWAs, offers both economic and environmental advantages by reducing landfill pressure and conserving natural resources [7].

Globally, biomass combustion for energy and heat production generates a substantial amount of ash, estimated at over 480–500 million tons per year, of which wood-derived residues represent a significant portion. Europe and North America remain leading regions in biomass energy utilization, while Asia, particularly China and India, has shown the fastest growth due to the gradual replacement of coal-fired systems with renewable alternatives [8,9]. Despite this, the majority of wood biomass ash is still landfilled or stored, largely due to compositional variability and the absence of standardized reuse frameworks. Recent reviews highlight that biomass ashes are rich in reactive oxides such as CaO, SiO_2, and K_2O, which can be effectively utilized in the production of construction materials, alkali-activated binders, or lightweight aggregates, thereby contributing to global circular economy targets and CO_2 reduction goals [10,11]. According to the International Energy Agency (IEA) Bioenergy report, improved classification and valorization of these ashes are essential to support sustainable waste management and carbon capture initiatives worldwide [12]. The valorization of WWFA in this study, therefore, not only addresses local Lithuanian waste management challenges but also aligns with the broader international shift toward low-carbon material production and biomass resource efficiency.

As technological progress continues and global urbanization accelerates, the construction sector experiences consistent growth. This expansion significantly increases the demand for key natural resources such as sand, gravel, and crushed stone. However, the overextraction of these materials has led to resource depletion, raising concerns about long-term environmental sustainability [13].

One promising solution is the replacement of natural aggregates with ALWAs made from industrial by-products, such as WWFA or wood bottom ash [14]. These recycled materials offer a sustainable alternative while reducing the environmental impact associated with raw material extraction. The global aggregates market is projected to exceed €500 billion by 2025. This growth is primarily driven by rising infrastructure investments in developing regions, particularly in the Asia-Pacific, the Middle East, and Africa [15]. Additionally, increased residential, commercial, and industrial construction projects worldwide are contributing to the expanding demand for aggregates. Nevertheless, the sector still faces several challenges. These include fluctuating raw material prices, stricter environmental regulations related to aggregate extraction, and potential disruptions in the supply chain [16].

The use of waste in the production of ALWAs has a promising future due to the growing interest and demand for recycling [15]. ALWAs made from waste have a positive impact on the environment, people, and the construction industry. The advantages of using waste materials can be summarized as follows: Firstly, the use of natural aggregates does not waste natural resources and avoids harmful aggregate extraction activities. Aggregates made from waste can be lighter than natural aggregates, resulting in lightweight concrete.

In addition, greenhouse gas emissions are reduced by reducing the need for large quantities of cement and the use of CO_2 gas for curing the aggregates by carbonization production, as well as reducing transport costs and emissions due to the lower density of the resulting material [17].

Many articles in the literature refer to the recycling of WWFA into building materials or fertilizers. Despite this, around 70% of the wood ash produced is still landfilled, with only 20% used as soil additives and 10% for other purposes. Wood ash contains various macro- and micro-nutrients as well as oxides, hydroxides, carbonates, and silicates that promote plant growth and can therefore be used as a soil fertilizer [18]. One of the parameters to be considered when using wood ash as a raw material is its chemical composition. Ash characteristics depend on the biomass type, combustion method, and the location of ash collection [19]. However, variability in composition poses challenges for consistent application. Beneficial oxides in WWFA, such as calcium oxide (CaO) and silica (SiO_2), can enhance concrete strength and durability through hydration, carbonation, and pozzolanic reactions forming calcium silicate hydrate (C–S–H) gel [20]. On the other hand, WWFA may also contain components like potassium oxide (K_2O), sodium oxide (Na_2O), and phosphorus pentoxide (P_2O_5), which can trigger alkali-silica reactions (ASR) or retard cement hydration, thereby reducing early strength [21].

Carbonation is a reaction between CO_2 and $Ca(OH)_2$, creating calcium carbonate, indicating the process of carbonation of the aggregates according to Equation (1) [22].

$$Ca(OH)_{2(s)} + CO_{2(g)} \rightarrow CaCO_{3(s)} + H_2O_{(l)} \tag{1}$$
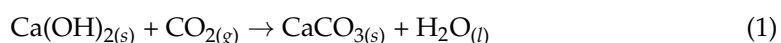
This equation represents the carbonation of hydrated lime under ambient conditions, where solid $Ca(OH)_2$ reacts with gaseous CO_2 to form solid $CaCO_3$ and liquid water.

Although industrial by-products such as slag and conventional coal-derived fly ash have been extensively explored in the production of ALWAs through carbonation-based methods, the potential of biomass-derived ashes, particularly WWFA, remains largely underexplored. Existing studies have demonstrated the effectiveness of fly ash in improving the mechanical and durability properties of concrete and aggregates, yet comparable investigations involving WWFA are still limited [23,24]. Given the growing volume of wood combustion by-products and the urgent need for sustainable construction materials, there is a clear research gap concerning the valorization of WWFA in aggregate production.

In this study, the carbonization method was used to produce ALWAs from WWFA in a CO_2 environment, and their mechanical and physical properties were investigated. ALWAs are of particular interest due to the significant accumulation of incineration waste in landfills. Their production not only facilitates waste reuse and recycling but also reduces greenhouse gas emissions through lower cement demand and CO_2-based curing technologies. Testing was conducted following the EN 13055:2016 standard for lightweight aggregates [13], which provided the basis for evaluating the mechanical and physicochemical properties of the aggregates that were produced in various compositions.

2. Materials and Methods

2.1. Materials

The WWFA used in this study was obtained from the UAB "Ekobazė" landfill, which handles Lithuanian industrial waste. Before the production of ALWAs, the ash was sieved using a fine mesh to remove foreign materials. Hydrated lime, which has good bonding properties when carbonized, was used as a binder to produce the ALWAs. The selected quantities of ash and lime were mixed and granulated gradually by adding water until the mixture began to granulate into small spherical pellets of different sizes. These ALWAs

were then stored at room temperature (20 °C and 60% RH) overnight before being placed in a carbonization chamber, where they were cured for 24 h.

The reference material used was commercial LECAs with a predominant size range of 4 to 16 mm, obtained from a building materials store. LECA was tested in parallel with the produced WWFA-based ALWAs under identical conditions. Reported values represent the mean $\pm$ SD of three repeated measurements. For compositional comparison, Table 1 summarizes the typical oxide composition of LECA obtained from literature and manufacturer data, which shows its high content of SiO_2 and Al_2O_3 compared with the CaO-rich WWFA. The compressive strength, bulk density, and water absorption of the reference material were 1.26 N/mm^2, 588.2 kg/m^3, and 21.1%, respectively. The chemical composition of the WWFA is given in Table 1. The total oxide content obtained by XRF accounts for approximately 85 wt%, which is typical for biomass-derived ashes. The remaining fraction is mainly attributed to carbon-containing compounds that are not detected by the XRF method. This was confirmed by X-ray diffraction (XRD) using a D8 Advance diffractometer (Bruker AXS, Karlsruhe, Germany), which identified calcite ($CaCO_3$) as one of the crystalline phases. Therefore, the difference is explained by the presence of carbonates and minor organic residues in the ash.

Table 1. Chemical composition of WWFA determined by X-ray Fluorescence (XRF) analysis.

	Chemical Composition											
	CaO	**K$_2$O**	**SO$_3$**	**SiO$_2$**	**MgO**	**P$_2$O$_5$**	**Al$_2$O$_3$**	**Cl**	**Fe$_2$O$_3$**	**TiO$_2$**	**Na$_2$O**	**Minor Chemical Compounds ***
WWFA (%)	37.8	12.9	11.4	9.4	4.6	3.9	1.8	1.7	1.4	-	-	1.4
LECA (%)	3.5	3	-	61.2	2.9	-	17.8	-	7.1	1.1	1.4	2

* LOI represents unburnt carbon, residual carbonates, and bound water. Minor chemical elements (e.g., Na$_2$O, TiO$_2$, MnO, ZnO, CuO, and others) were <0.1% each. Trace elements below 0.5 wt% were detected but not included in the major chemical composition summary. LECA data compiled from manufacturer technical sheets and previous analyses of sintered expanded clay aggregates [25,26].

The three different compositions of WWFA and binder (slaked lime, $Ca(OH)_2$) used in this study were selected based on previous research findings and the optimization of the binder–ash ratio (Table 2). In each case, the binder content was reduced by approximately 6.25% to produce three distinct mixtures, labeled A0.32 L, A0.30 L, and A0.28 L. These compositions are defined by the ratio of WWFA to $Ca(OH)_2$, where A0.32 L has the highest binder content (32%), A0.30 L contains 30% binder, and A0.28 L has the lowest binder content (28%). In addition, the water-to-mixture (w/m) ratio for each composition is 0.25, 0.38, and 0.35, respectively.

Table 2. Mixtures for the manufacture of ALWAs.

Composition	Wood Waste Ash (g)	Binder (g) Ca(OH)$_2$	Water (g)	w/m	4/16 Fraction (g)	16/32 Fraction (g)	4/16 Fraction Yield (%)	16/32 Fraction Yield (%)	0/4 Fraction (g)	>32 Fraction (g)	0/4 Fraction Yield (%)	>32 Fraction Yield (%)
* A0.32 L	5000	1600	1650	0.25	1660.0	3812.9	25.15	57.77	74.1	1053.36	1.12	15.96
** A0.30 L	5000	1500	2470	0.38	2791.7	3446.5	42.95	53.02	37.4	224.25	0.58	3.45
*** A0.28 L	5000	1400	2240	0.35	4125.3	2258.4	64.46	35.29	8.2	7.68	0.13	0.12

* A0.32 L-Mixture with 32% binder (Ca(OH)$_2$) and 68% WWFA.; ** A0.30 L-Mixture with 30% binder and 70% WWFA; *** A0.28 L-Mixture with 28% binder and 72% WWFA. Water mass was excluded from calculations, as it evaporates during granulation and curing. Reported masses and yields are based on post-carbonation, oven-dry aggregates (105 °C, 24 h).

The binder content in these mixtures influences the properties of the aggregates, such as strength, porosity, and workability. A0.32 L provides the highest binder proportion,

which leads to a relatively dense aggregate structure, requiring less water for granulation. In contrast, A0.30 L and A0.28 L, with reduced binder contents, require more water to achieve similar granulation characteristics. This is evident in the granulation process, where the water demand increases as the binder content decreases, affecting both the granule formation and the final aggregate properties.

Furthermore, granulation of the compositions with varying WWFA and $Ca(OH)_2$ ratios revealed that the ratio significantly affects the water demand during granulation. When the binder content is higher (as in A0.32 L), relatively less water is needed for granulation. However, reducing the lime content (as in A0.30 L and A0.28 L) leads to an increased requirement for water to produce aggregates of similar dimensions. This change in water demand is crucial for controlling the quality and consistency of the ALWAs.

Since the 4/16 fraction of aggregates is more commonly used in construction, the focus of this study is placed on analyzing this fraction, ensuring the results apply to practical applications in the construction industry.

It should be noted that direct comparison of crushing resistance between WWFA-based aggregates and LECA may not reflect their true structural performance, as these materials differ significantly in bulk density. Therefore, the structural quality coefficient (SQI), defined as the ratio of crushing resistance (f_a) to bulk density (ρ_b), was introduced to evaluate the mechanical efficiency of the aggregates. This approach allows for density-normalized comparison.
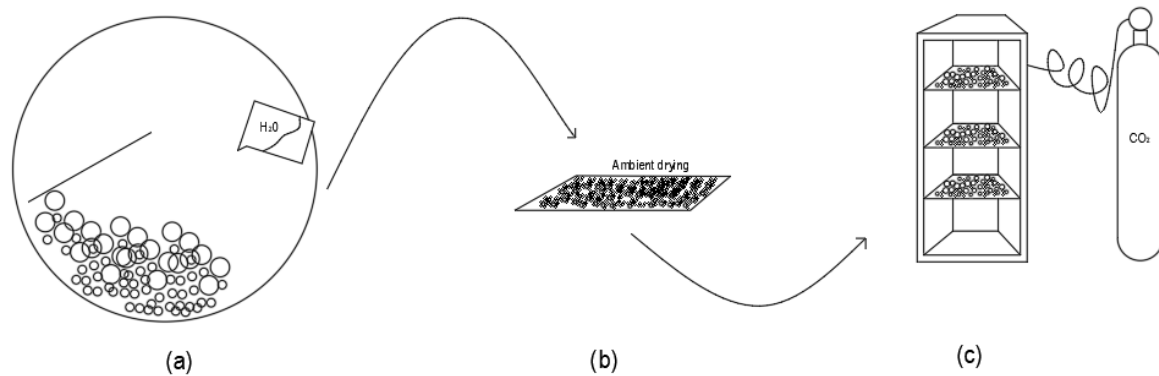
2.2. Granulation Process

We clarified that size fractions were determined according to EN 933-1 [27], and that all masses and yields were calculated on a post-carbonation, oven-dry basis (105 ± 5 °C, 24 h). The added water was not included in the mass balance, and a slight increase in total mass is attributed to CO_2 uptake during carbonation. WWFA was combined with three different binder compositions, corresponding to 30%, 32%, and 34% of the WWFA mass (Table 2). The granulator used in this study had a diameter of 1000 mm and a depth of 300 mm, operating at a fixed rotational speed of 25 rpm and an angle of 45°.

The WWFA and lime were mixed in a dry container before being transferred to the granulator drum. Water was gradually added as the mixture rotated until nuclei began to form. Due to differences in composition, each mixture required a slightly different amount of water. The palletization process continued until granules of varying sizes were fully formed. The resulting aggregates from all mixtures were collected and left to dry at ambient room temperature for 24 h. This was followed by a curing process known as carbonation, in which the pellets were placed in a carbonation chamber for another 24 h to harden under controlled CO_2 exposure (20 °C, 64% RH, 19% CO_2 concentration). Figure 1 illustrates the granulation and curing stages, including (a) granulation in the disk granulator, (b) ambient drying, and (c) hardening in the carbonation chamber.

2.3. Hardening Conditions

The curing of the produced aggregates was performed in a specialized scientific carbonization chamber, as shown in Figure 2. The chamber had open shelves to ensure uniform exposure and carbonization of all samples. The carbonization process was conducted under controlled conditions: a temperature of 20 °C, 64% relative humidity, and a CO_2 concentration of 19%. All ALWAs remained in the chamber for 24 h. After carbonization, the samples were removed and stored at room temperature until further testing and analysis.

Figure 1. Granulation and Curing process: (**a**) Granulation in disk granulator, (**b**) Ambient curing, and (**c**) Hardening in carbonation chamber.

Figure 2. Carbonization of aggregates in a special chamber.

2.4. Resistance to Crushing

A Toni Technik 2020 hydraulic press (Toni Technik Baustoffprüfsysteme GmbH, Berlin, Germany) was used for the splitting resistance test, as shown in Figure 3. This test followed the procedure defined in EN 1097-11 [28], which specifies the method for measuring the resistance of lightweight aggregates to compressive loading. The term "resistance to crushing" used throughout this manuscript corresponds to this standardized compressive resistance test. The fragmentation resistance test described in EN 1097-2 [29] (Los Angeles method) was not applied, as the produced cold-bonded aggregates were assessed primarily for compressive-type failure behavior. The maximum force of the specimens was measured after 2 days, and the specimens were placed in a steel test cylinder specially designed for the specimens, which was pressed with a piston adapted to the cylinder. The ALWAs used for the test were of the 4/16 fraction, and the crushing strength was calculated according to Equation (2) for each specimen composition [13,28]:

$$C = \frac{L + F}{A} \, \text{N/mm}^2; \tag{2}$$

where *C* is the crushing resistance (N/mm²), F is the maximum load (force) applied to the aggregate specimen at failure, *A* is the loaded area of the piston (mm²), and *L* is the applied load level corresponding to the peak force. The value of *F* corresponds to the maximum compressive load recorded before visible particle fracture or a sharp load drop, representing the failure point of the aggregate under compression.

Figure 3. (**A**) Hydraulic press, (**B**) pressing cylinder, (**C**) samples in the crushing cylinder, and (**D**) crushed aggregates removed from cylinder.

2.5. Apparent Density, Specific Density, Bulk Density, Water Absorption, and Porosity

To produce ALWAs, they must meet the basic requirements of EN 13055:2016, that the particle density does not exceed 2000 kg/m³ or the bulk density does not exceed 1200 kg/m³ [13]. Therefore, all produced compositions were weighed, and their particle and bulk densities were calculated according to EN 1097-3 [30] and water absorption according to EN 1097-6 [31] using Equations (3)–(5):

Particle density:

$$\rho_b = \frac{m_a}{m_a - m_w} \times \rho_w \tag{3}$$

where m_a is the mass of the sample in air, in grams (g), m_w is the mass of the sample in water, in grams (g), and ρ_w is the density of water at the test temperature, in megagrams per cubic meter (Mg/m³).

Bulk density:

$$\rho_b = \frac{m_2 - m_1}{V} \tag{4}$$

where ρ_b is bulk density, in megagrams per cubic meter (Mg/m³), m_2 is the measuring vessel and the sample, in kilograms (kg), m_1 is the mass of the empty measuring vessel, in kilograms (kg), and *V* is the volume of the measuring vessel, in liters (L).

Specific density:

$$\rho_d = \frac{(m - m_1) \times \rho_w}{m - m_1 + m_2 - m_3} \tag{5}$$

where *m* is the mass of the pycnometer with powder, in grams (g), m_1 is the mass of the empty pycnometer, in grams (g), m_2 is the mass of the pycnometer with distilled water, in

grams (g), m_3 is the mass of the pycnometer with distilled water and powder, in grams (g), and ρ_w is the density of water depending on air temperature, in kilograms per cubic meter (kg/m^3).

Porosity:

Porosity is calculated according to the European standard EN 1097-3 [30] as in Equation (6).

$$P = \left(1 - \frac{\rho_b}{\rho_d}\right) \times 100 \tag{6}$$

where P is the porosity of the sample in percent (%), ρ_b is the particle density of the sample, ρ_d is the specific density of the sample.

Water absorption:

Water absorption (*WA*) was calculated using Equation (7):

$$WA = \frac{Wet\ weight - Dry\ weight}{Dry\ weight} \cdot 100 \tag{7}$$

where the mass of wet aggregates is the mass of aggregates soaked in water after 24 h, and the mass of dry aggregates is the mass of aggregates dried in an oven at 105 °C for 24 h.

All experimental measurements (particle density, bulk density, water absorption, crushing resistance, and freeze–thaw mass loss) were performed in triplicate (n = 3). The reported results are expressed as mean ± standard deviation (SD), and the corresponding error bars represent these SD values.

2.6. Chemical Analysis

XRD and X-ray fluorescence (XRF) using a fluorescence spectrometer S8 Tiger (Bruker AXS, Karlsruhe, Germany), both techniques were used to analyze the chemical properties of the samples. These methods were used to assess the chemical composition of all ALWAs produced, identifying the predominant chemical elements and compounds present. XRD analysis was used to determine the mineral phases that formed either during wood combustion or the aggregate production process. It also helped evaluate the effectiveness of the carbonization process by identifying the presence of stable carbonate phases. The XRF technique was applied to detect the elemental and oxide composition of the WWFA, identifying components that may be either beneficial or negative in construction applications.

The results of XRF shown in Table 1 revealed that the primary component of the WWFA is calcium oxide (CaO), which enhances the carbonization activity and contributes significantly to the strength development of the aggregates. The ash also contained notable amounts of SO_3, K_2O, and SiO_2, elements known to improve both the chemical stability and mechanical performance of cementitious materials.

XRD analysis of WWFA, illustrated in Figure 4, confirmed the presence of well-defined crystalline phases, including calcite ($CaCO_3$) at approximately 30° 2θ and quartz (SiO_2) at approximately 27° 2θ. The strong diffraction peaks corresponding to calcite indicate successful carbonation of the aggregates. The detection of quartz reflects the persistence of siliceous phases in the ash. Additionally, weak diffraction peaks corresponding to Portlandite ($Ca(OH)_2$) were identified, which likely originate from hydration of free lime (CaO) during post-combustion cooling and storage, rather than from primary formation in the combustion process. Such secondary portlandite formation is commonly observed in biomass fly ashes rich in calcium oxides and exposed to ambient humidity [2,18]. Overall, the XRD data suggest that the carbonation process is highly effective in transforming the WWFA's mineral phases, contributing to improved mechanical strength and stability of the final ALWAs.
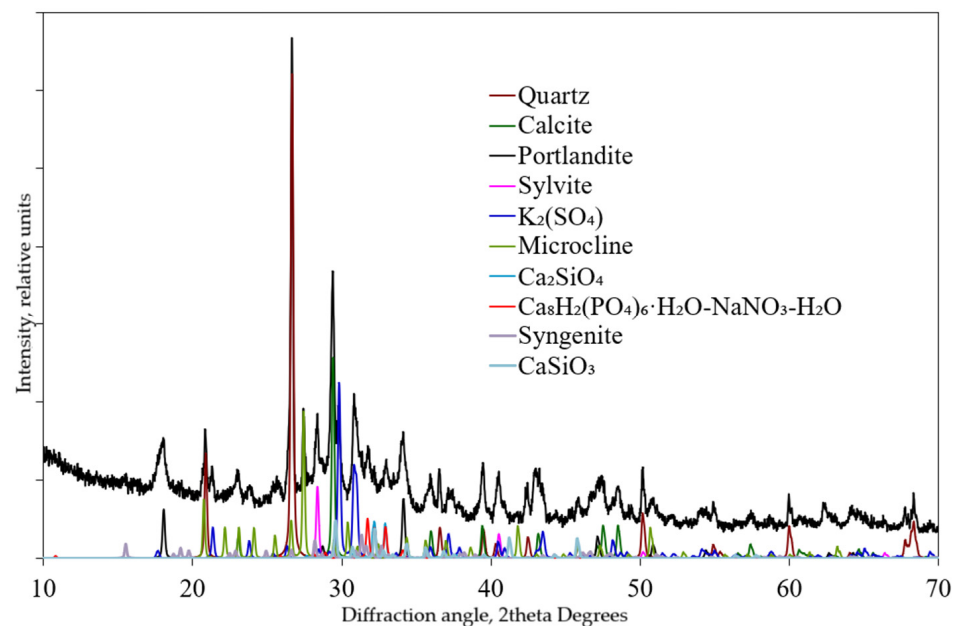
Figure 4. XRD pattern of the raw WWFA, showing predominant crystalline phases of calcite ($CaCO_3$) and quartz (SiO_2), along with minor portlandite ($Ca(OH)_2$) reflections.

Scanning Electron Microscopy (SEM) analysis was performed using a ZEISS EVO MA10 microscope (Carl Zeiss AG, Oberkochen, Germany). SEM methodology was employed to analyze the microstructure of the ALWAs produced from WWFA. This method provided high-resolution visualization of the physical characteristics of the aggregates at the microscale, essential for evaluating their structural quality and potential behavior in concrete. Images were captured to observe surface morphology, particle bonding, pore structure, and microcracks.

2.7. pH Level Determination

pH adjustment after carbonization is an important consideration when using aggregates in building materials. For this test, aggregates from each formulation were ground into a fine powder and mixed with distilled water in a flask. After allowing the ash particles to settle, the pH level of the solution was measured [2].

Based on pH values and the calcium-to-sulfur ratio, fly ash can be classified into three categories:

- Acidic ash (pH 1.2–7).
- Mildly alkaline ash (pH 8–9).
- Strongly alkaline ash (pH 11–13).

This classification helps assess the potential reactivity and suitability of the ash for use in various construction applications. Additionally, the pH level can be used to assess the effectiveness of carbonation in the aggregate, i.e., to determine whether the binder has fully carbonated.

2.8. Freezing and Thawing Resistance of Lightweight Aggregates

The freeze–thaw resistance of ALWAs is crucial for the resistance of the final product (concrete) to environmental influences, and more specifically to cyclic freezing and thawing. The porosity, moisture content, and presence of air-retentive materials in the aggregates are among the main criteria for resistance to freezing and thawing.

In this study, the refrigeration and defrosting test was carried out in accordance with the European Standard EN 1367-7 [32]. The prepared compositions with comparative Leca

were placed in specially prepared metal containers containing 0.5 L or 1 L of samples according to the granulometric composition. The samples were then immersed in water at atmospheric pressure and subjected to 20 cycles of cooling and thawing. The samples were first cooled to −17.5 °C in air and then thawed in a water bath to about 20 °C. When all cycles were completed, the mass loss was calculated according to Equation (8) [32].

$$FL_I = [(M_1 - M_2)/M_1] \times 100 \qquad (8)$$

where FL_I is the percentage loss in mass of the test specimen, M_1 is the initial dry mass of the test specimen before freeze–thaw cycling in grams (g), and M_2 is the final dry mass of the test specimen after freeze–thaw cycling that is retained on the specified sieve, in grams (g).

2.9. Statistical Analysis

All experimental results were based on triplicate tests (n = 3) and are expressed as mean ± standard deviation (SD). Statistical analysis was performed using one-way analysis of variance (ANOVA) to determine significant differences among mixtures (A0.32 L, A0.30 L, A0.28 L) and between each ALWA and the commercial LECA reference. Differences were considered statistically significant when $p < 0.05$.

3. Results and Discussion

3.1. Results for Particle Density, Bulk Density, and Water Absorption

The particle and bulk density results of the produced ALWAs confirm their classification as lightweight aggregates according to the relevant standards (Figure 5). As shown in Figure 5, all samples exhibited bulk densities below 1200 kg/m³, specifically ranging from 1010.9 to 1060.0 kg/m³, indicating their suitability for use in lightweight construction materials.
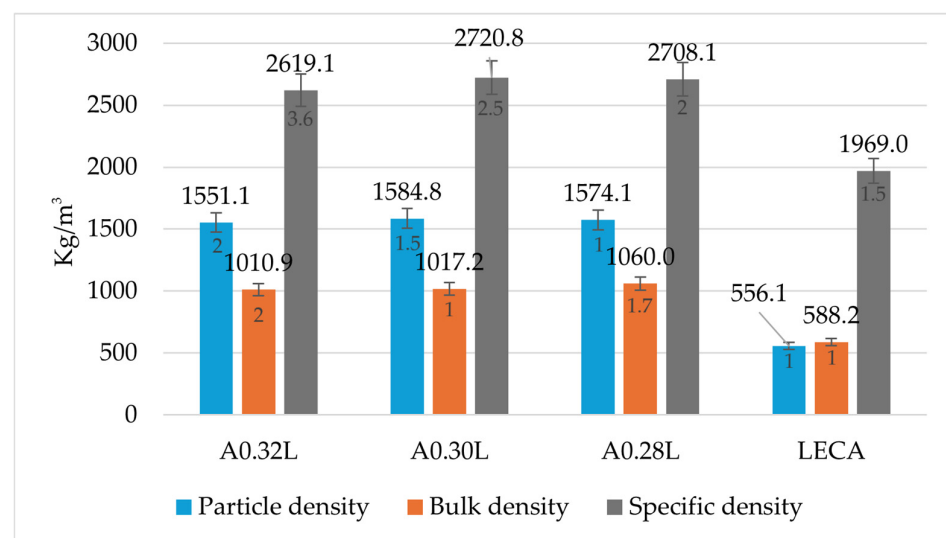

Figure 5. Comparison of particle density, bulk density, and specific density of ALWAs and LECA (mean ± SD, n = 3). Error bars represent ± standard deviation of three replicate measurements.

The apparent particle densities of the aggregates also remained well below the 2000.0 kg/m³ threshold, with values between 1551.1 kg/m³ and 1584.8 kg/m³ for the ash-based samples. For comparison, the LECA showed significantly lower particle (556.0 kg/m³) and bulk (588.2 kg/m³) densities, as expected due to its highly porous structure.

Interestingly, the specific density values for the ALWAs ranged from 2619.1 kg/m^3 to 2720.8 kg/m^3, while LECA showed a much lower specific density of 1969.0 kg/m^3. This indicates that although LECA is lighter overall, the denser matrix of the ash-based samples may offer mechanical benefits depending on the application. The observed trend suggests that increasing binder Ca(OH$_2$) content correlates with reduced density values, likely due to the influence of ash on pore formation during granulation. This porous internal structure contributes to the lower density of the aggregates, which is advantageous for reducing the structural load in construction. These results align well with previous studies. For example, Dong et al. [33] reported bulk densities of 1043–1080 kg/m^3 for ALWAs made from fly ash and a blended sodium silicate/hydroxide solution. Similarly, Chi et al. [25] observed bulk densities ranging from 850 to 970 kg/m^3 in cold-bonded aggregates containing cement binders. Thus, the bulk densities achieved in this study are comparable to those in other established research, further supporting the potential application of these wood ash-based aggregates in lightweight concrete production.

Water absorption is a key indicator of the porosity and durability of lightweight aggregates. As shown in Figure 6, all experimental samples exhibited higher water absorption values compared to commercial LECA, which recorded a value of 21.1%. Among the produced aggregates, sample A0.28 L showed the highest absorption at 25.1%, indicating a more porous internal structure. A0.32 L and A0.30 L had similar absorption values of 23.5% and 23.6%, respectively. These results suggest that while the developed aggregates are slightly more porous, they still meet performance expectations for applications where moderate absorption is acceptable. Further optimization of the mix design or curing conditions could reduce porosity and improve water resistance. Shen et al. utilized waste concrete powder as the primary raw material to manufacture artificial aggregates, with recycled concrete powder content ranging from 70% to 90%. The results indicate that the aggregate has water absorption rates between 6.3% and 26% [34].
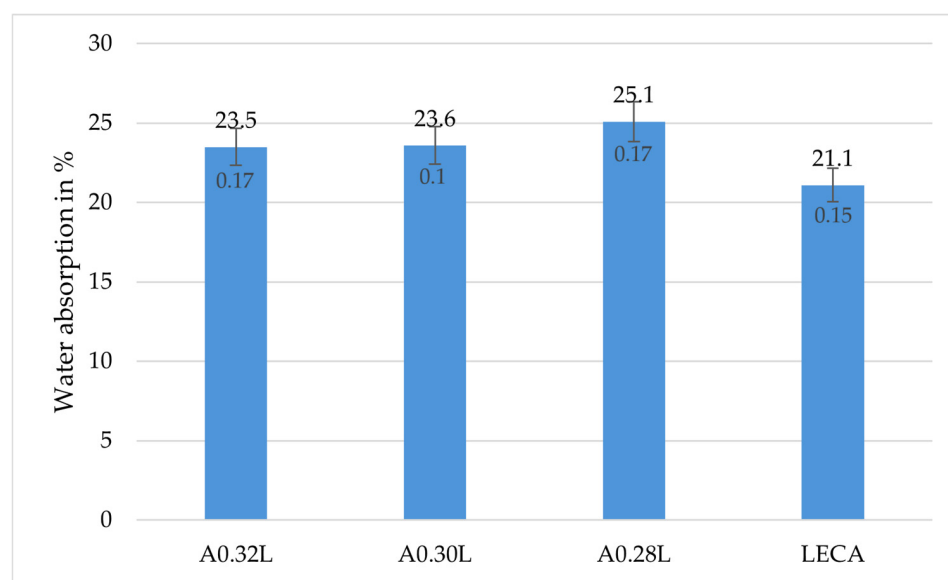
Figure 6. Water absorption (%) of ALWAs compared to LECA (mean ± SD, n = 3). Error bars represent ± standard deviation of three replicate measurements.

The chemical composition of the WWFA and the binder strongly affects the water absorption behavior of the produced aggregates. During carbonation, Ca(OH)$_2$ reacts with CO$_2$ to form CaCO$_3$, which densifies the microstructure and reduces the open porosity. Consequently, the lime content and the water-to-mixture ratio play a major role in determining the final pore structure and, therefore, the absorption capacity of the aggregates.

In contrast, the intrinsic microstructure of WWFA particles, developed during wood combustion, primarily defines the initial texture of the granules before carbonation. The final water absorption is mainly governed by the extent of lime carbonation and the proportion of WWFA in the mixture, both of which influence the balance between compact carbonate phases and residual porous regions.

3.2. pH Levels Determination

Determining the pH of fly ash aggregates is essential for assessing their chemical reactivity, compatibility with cementitious systems, and overall durability [10]. Additionally, pH plays a critical role in evaluating the environmental safety of fly ash use, as it influences the leaching behavior of potentially hazardous elements [35]. Therefore, pH measurement serves as a key parameter in both quality control and performance prediction [5]. Results of manufactured aggregates and WWFA itself are shown in Table 3.

Table 3. pH levels, results, and porosity of samples of carbonized aggregates.

| Composition	pH Level	Porosity, %
WWFA	12.21	-
A0.32 L	11.66	40.77
A0.30 L	12.09	41.75
A0.28 L	10.42	41.88
LECA	9.70	71.76

The pH levels of the raw WWFA and the manufactured aggregates are presented in Table 3. Among the tested materials, WWFA exhibited the highest pH value (12.21), followed closely by A0.28 L (12.09). The pH levels of A0.32 L and A0.30 L were 11.66 and 10.42, respectively. In comparison, the LECA sample showed a lower pH of 9.70, indicating a less alkaline nature. These results are consistent with findings in the literature. These high pH values are consistent with other studies on wood ash and biomass ashes: for example, a study by Ercan et al. reported that wood ash typically has pH values in the range of 9–13.5, owing to its content of hydroxides, carbonates, and free lime [11]. Another recent review by Martínez-García et al. similarly noted that ashes from wood combustion are highly alkaline, that is, in the same high pH range, reinforcing that WWFA behaves in line with typical biomass ash chemistry [36]. Together, these studies support our findings, suggesting that the WWFA and some manufactured aggregates in our study do reach high alkalinity levels that are relevant for assessing both their performance (via binder carbonation, delayed hydration) and environmental safety.

The combined XRD patterns of the A0.32 L, A0.30 L, and A0.28 L compositions of ALWA are presented in Figure 7. All mixtures show predominant crystalline phases of calcite ($CaCO_3$) and quartz (SiO_2).

Additional XRD analysis of the raw WWFA confirmed the presence of calcium silicates (Ca_2SiO_4, $CaSiO_3$) and potassium sulfate (K_2SO_4), indicating that these phases were already present in the ash before granulation. Therefore, their detection in the carbonated aggregates originates from the precursor material rather than from secondary reactions during curing [37]. The short carbonation curing duration (24 h) likely limited the formation of calcium hydrosilicates, which typically develop under longer hydration conditions. In addition, organic impurities present in WWFA may have further delayed or inhibited the hydration of calcium silicate phases.

Increasing the binder ($Ca(OH)_2$) content enhanced the intensity of calcite peaks (notably near 29.4° 2θ), confirming more extensive carbonation in the A0.32 L mixture. In

contrast, the lower-binder formulations (A0.30 L, A0.28 L) exhibited relatively reduced calcite intensities but stable quartz peaks, reflecting the inert nature of siliceous components. The combined presentation enables clearer comparison of these relative phase evolutions across compositions. These results demonstrate that variations in lime content influence the extent of carbonation and the balance between crystalline and amorphous phases in the produced ALWAs.
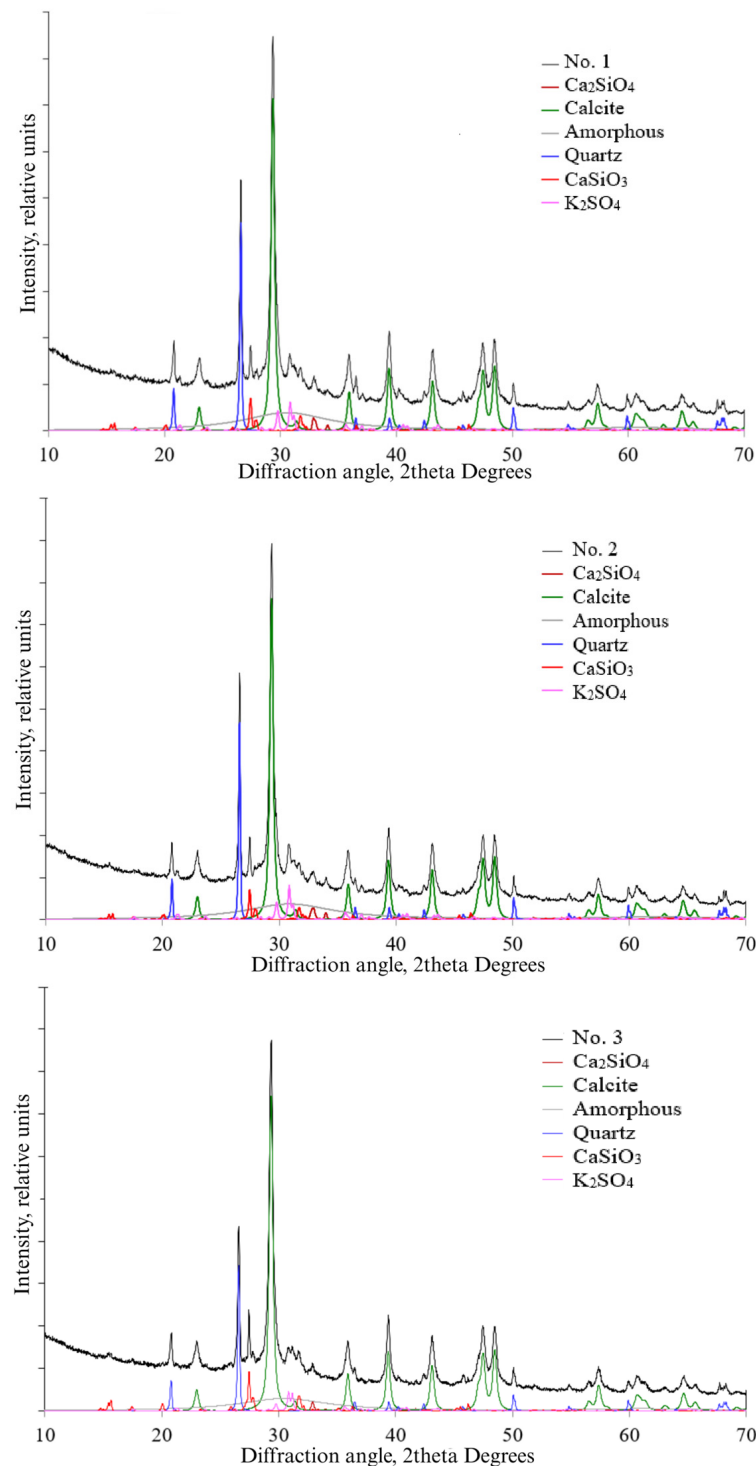
Figure 7. Combined XRD patterns of ALWA compositions: A0.32 L (No. 1), A0.30 L (No. 2), A0.28 L (No. 3). The diffractograms illustrate the relative intensities of calcite ($CaCO_3$), quartz (SiO_2), and secondary calcium hydrosilicate (C–S–H–type) phases that formed during carbonation.

The relatively high K_2O content (12.9%) in the WWFA primarily corresponds to the presence of potassium sulfate (K_2SO_4), as confirmed by XRD. Although elevated potassium levels may promote alkali–silica reactions or accelerate setting in cementitious systems, in this study, no pre-treatment or removal of K_2O was carried out in order to evaluate the ash in its as-received, industrially relevant form. Despite the presence of sulfates, the produced aggregates exhibited stable alkaline pH values (10.4–12.2), indicating good chemical stability and environmental safety. From a practical standpoint, neutralizing or removing the K_2SO_4 component would be economically inefficient and unnecessary for this application.

3.3. Resistance to Crushing of Aggregates

The mechanical performance of the produced aggregates was evaluated in terms of both their crushing resistance and corresponding structural quality coefficient (SQI), defined as the ratio of crushing resistance (f_a) to bulk density (ρ_b). This normalization accounts for density differences between WWFA-based ALWAs and LECA, providing a more accurate comparison of strength-to-weight efficiency. The crushing resistance values and calculated SQI are summarized in Table 4 and illustrated in Figure 8. Statistical analysis confirmed that the differences in crushing resistance among ALWA compositions were significant ($p < 0.05$), with A0.28 L showing the highest strength-to-weight efficiency. All WWFA-based aggregates also differed significantly from LECA ($p < 0.001$).

Table 4. Structural quality coefficient (SQI = strength/bulk density) of ALWAs and LECA.

Composition	Crushing Resistance (N/mm^2)	Bulk Density (kg/m^3)	SQI ($\times 10^{-3}$ N·mm^{-2}·m^3·kg^{-1})
A0.32 L	2.41	1010.9	2.38
A0.30 L	1.90	1017.2	1.87
A0.28 L	2.74	1060.0	2.58
LECA	1.26	588.2	2.14

The SQI reflects the strength-to-weight efficiency of the aggregates; higher values indicate better structural performance.
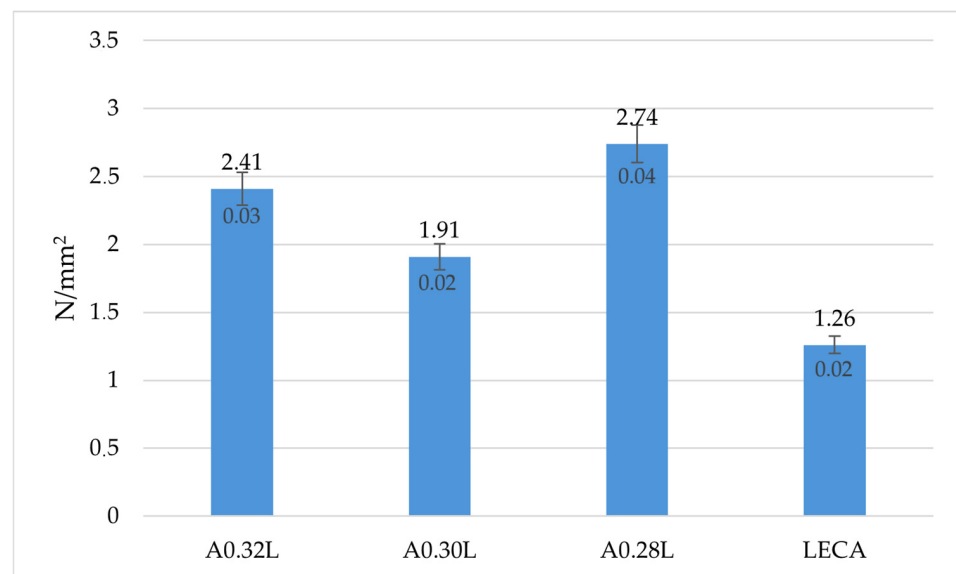
Figure 8. Crushing resistance of ALWAs and LECA (mean ± SD, n = 3). Error bars represent ± standard deviation of three replicate measurements.

The results (Table 4) show that all tested samples demonstrated higher absolute crushing resistance compared to LECA; however, due to their higher bulk densities, a direct comparison can be misleading. When expressed through the structural quality coefficient, A0.28 L achieved the highest SQI value (2.58×10^{-3}), confirming its superior strength-to-weight performance. The comparable SQI of LECA (2.14×10^{-3}) reflects its low density despite lower strength, highlighting the usefulness of this normalized metric. Among the tested formulations, A0.28 L demonstrated the highest resistance (2.74 N/mm^2), indicating a stronger internal structure, likely due to optimal binder interaction and reduced porosity. A0.32 L and A0.30 L followed with values of 2.41 and 1.90 N/mm^2, respectively. These findings confirm that wood ash-based lightweight aggregates can achieve superior mechanical strength compared to conventional lightweight materials, enhancing their potential for structural applications. One of the key factors contributing to this performance is the carbonation curing process. After granulation, aggregates were initially brittle and could be crushed by hand. However, once cured in the carbonation chamber, the reaction between hydrated lime ($Ca(OH)_2$) and CO_2 gas formed calcium carbonate ($CaCO_3$), which filled pores, bonded the ash particles, and hardened the surface. This chemical process is described by Equation (8) and has been shown to significantly enhance compressive strength.

Similar improvements were observed by Lin et al. [26], who reported that incorporating wood biomass ash into cold-bonded fly ash aggregates enhanced their strength due to pore refinement and improved binder–ash interaction. Viola et al. [38] also confirmed that carbonation of wood ash significantly increased mechanical performance, with $CaCO_3$ precipitation densifying the microstructure, consistent with the enhanced resistance after carbonation curing. Moreover, Tripathi et al. [39] demonstrated that partial replacement of cement with hardwood biomass ash, combined with carbonation, yielded compressive strengths comparable to reference concretes, highlighting the potential of wood ash to provide structural performance without compromising durability. These parallels indicate that the superior resistance to crushing achieved in the current work is largely attributable to the synergistic effects of lime addition and carbonation, which are in agreement with broader findings on wood ash utilization in construction materials. These findings align with previous research using WWFA for lightweight aggregate production [4,12,14], where carbonation curing and optimized binder ratios significantly improved mechanical efficiency.

3.4. Resistance to Freezing and Thawing

One of the critical parameters for evaluating the durability of ALWA is its performance under freeze–thaw conditions. Figure 9 presents the mass loss (%) of different aggregate samples–A0.32 L, A0.30 L, A0.28 L, and LECA–after 20 repeated freezing and thawing cycles. The variation in freeze–thaw mass loss among the ALWA compositions was statistically significant ($p < 0.05$), confirming the superior durability of A0.28 L compared with A0.30 L and A0.32 L. The results show that A0.28 L had the best freeze–thaw performance among the experimental samples, with a mass loss of 6.19%, followed by A0.32 L at 7.13%. The A0.30 L sample exhibited the highest deterioration, with a mass loss of 9.46%, indicating reduced durability. In contrast, the reference LECA sample demonstrated superior resistance to freeze–thaw cycling, showing a negligible mass loss of only 0.70%. Although the LECA performed significantly better, the ALWAs produced from WWFA still maintained moderate resistance, making them suitable for non-structural or moderately exposed environments. In addition to physical durability, the chemical stability of the carbonated aggregates was evaluated qualitatively. The WWFA used contained low concentrations of chlorine (1.7 wt%) and trace heavy metals (Pb, Zn, Cu, Cr < 0.1 wt%),

consistent with previous analyses of biomass ashes. During carbonation, these ions are effectively immobilized by the formation of insoluble carbonates and encapsulation within the $CaCO_3$-rich binder matrix. Similar stabilization effects were reported by Tesovnik et al. and Viola et al. [23,38], confirming the ability of carbonation to reduce metal leachability. No visible efflorescence or mass loss associated with salt migration was observed, indicating good retention of soluble species. Thus, while LECA is chemically inert due to sintering, the WWFA-based ALWAs can be considered environmentally safe for non-structural applications, with limited risk of contaminant release. These results suggest that durability could be further enhanced through optimization of binder content, curing methods, or aggregate fraction size.
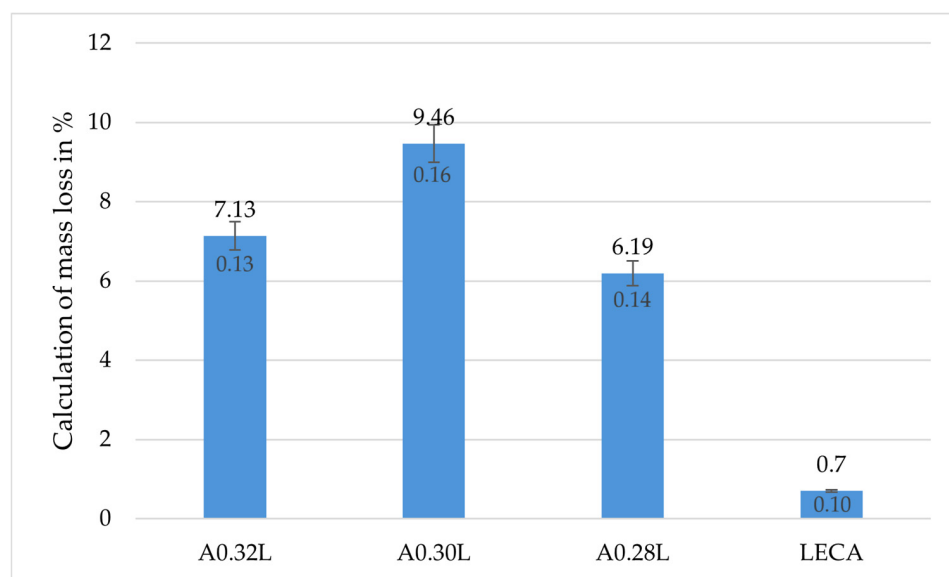
Figure 9. Freeze–thaw mass loss of ALWAs and LECA (mean $\pm$ SD, n = 3). Error bars represent $\pm$ standard deviation of three replicate measurements.

3.5. Microstructure of the Granules

Figure 10 presents SEM images of ALWAs produced with different water-to-mixture (w/m) ratios and a constant amount of WWFA, alongside commercial expanded clay aggregate (LECA) for comparison. Image A (A0.32 L, w/m = 0.25) shows a dense microstructure with limited pores, resulting from low w/m and high binder content. Image B (A0.30 L, w/m = 0.38) reveals higher porosity with visible voids and microcracks, while Image C (A0.28 L, w/m = 0.35) displays the most pronounced porosity due to the lowest binder dosage. Image D (LECA) shows a highly porous structure with large spherical voids typical of sintered aggregates. Overall, ALWAs exhibited finer pore structures than LECA, with porosity largely governed by the w/m ratio and binder content.

Figure 11 shows SEM micrographs of ALWAs, illustrating detailed surface morphologies and evidence of calcium carbonate ($CaCO_3$) crystal formation. In sample A0.32 L (Figure 11A), the dense microstructure with limited pores shows localized $CaCO_3$ deposits, indicating that the high binder content (1600 g $Ca(OH)_2$) promoted effective carbonation and pore filling. The A0.30 L sample (Figure 11B) exhibited a more porous and uneven surface, with scattered carbonate crystals, aligning with decreased binder efficiency due to a higher w/m ratio (0.38). In A0.28 L (Figure 11C), distinct needle-like $CaCO_3$ crystals were visible within the matrix, indicating precipitation inside voids and on unreacted ash surfaces; however, the lower binder amount (1400 g $Ca(OH)_2$) limited overall densification. In contrast, the reference LECA sample (Figure 11D) showed a smooth, sintered surface with

spherical pores and little evidence of carbonate precipitation, emphasizing the differences between sintered and cold-bonded aggregates.

These observations confirm that carbonation curing effectively induced $CaCO_3$ crystallization within ALWA matrices, improving particle bonding and potentially contributing to the higher crushing resistance reported in Figure 8. The distribution and morphology of crystals were strongly influenced by the water-to-binder ratio and binder dosage, with denser structures forming at low w/m ratios and higher lime contents.
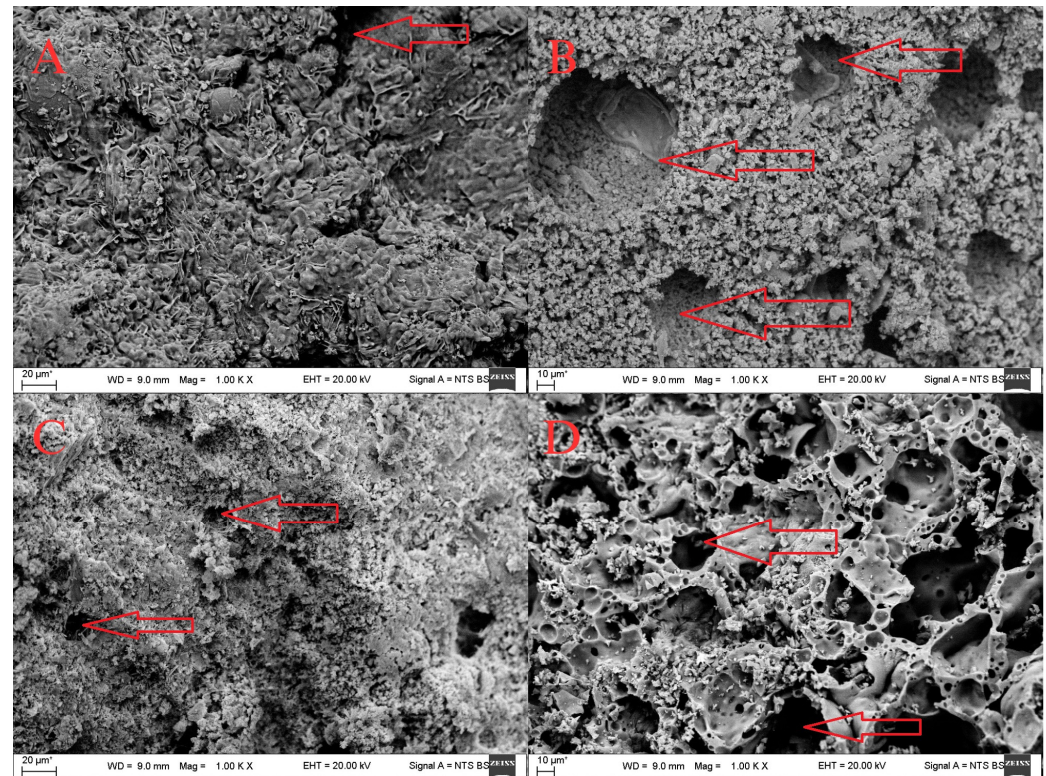
Figure 10. SEM micrographs of ALWAs with different compositions, illustrating variations in pore structure. (**A**) A0.32 L (w/m = 0.25, 1600 g $Ca(OH)_2$) shows a dense microstructure with limited pores; (**B**) A0.30 L (w/m = 0.38, 1500 g $Ca(OH)_2$) exhibits increased porosity and visible microcracks; (**C**) A0.28 L (w/m = 0.35, 1400 g $Ca(OH)_2$) shows pronounced voids; (**D**) Commercial expanded clay aggregate (LECA). Red arrows indicate pores. Magnifications: 1000×. The asterisk (*) indicates that the scale bars (10 μm or 20 μm) were automatically generated by the SEM software (Zeiss NTS system) and represent the true magnification for each image.

The SEM results (Figures 10 and 11) show that carbonation and binder content strongly influence ALWA microstructure. Low w/m mixtures (A0.32 L) developed denser, more cohesive surfaces with $CaCO_3$ crystals filling pores, while higher w/m ratios (A0.30 L, A0.28 L) exhibited more open structures with scattered or needle-like carbonate deposits. This densification through carbonation explains the higher crushing resistance of ALWAs compared to LECA. Similar effects were reported by Morandeau et al. [40] in OPC–fly ash systems. Tesovnik et al. [23] also observed improved stability in biomass fly ash aggregates after carbonation, while Lin et al. [26] and Tripathi et al. [39] confirmed that wood/biomass ash aggregates benefit from $CaCO_3$ precipitation, achieving enhanced strength and durability. Together, these findings support that carbonation-induced calcite formation is the key mechanism for improving WWA-based aggregate.
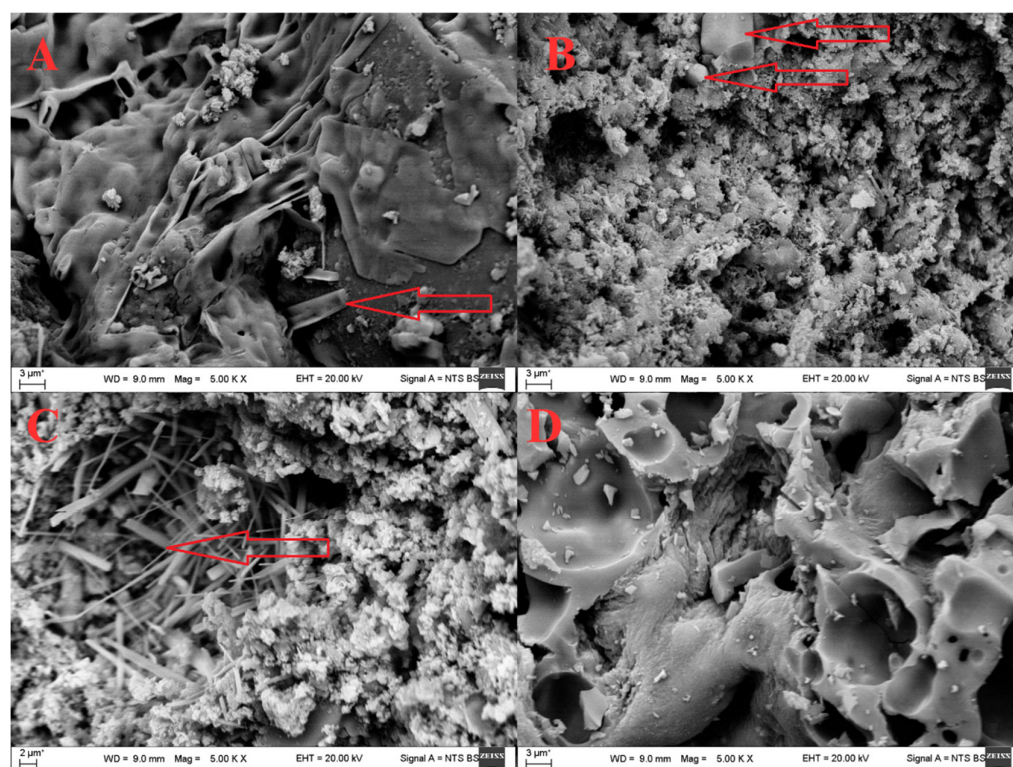
Figure 11. SEM micrographs of ALWAs at higher magnification (5000×), highlighting surface morphology and carbonate crystal formation. (**A**) A0.32 L (w/m = 0.25) shows dense surfaces with localized $CaCO_3$ crystal deposits; (**B**) A0.30 L (w/m = 0.38) reveals a porous structure with scattered crystal formation; (**C**) A0.28 L (w/m = 0.35) displays needle-like $CaCO_3$ crystals embedded within the matrix; (**D**) commercial LECA shows a smooth sintered surface with minimal evidence of carbonate crystallization and with large spherical pores. Arrows indicate key microstructural features, including carbonate deposits. Magnification: 5000×. The asterisk (*) indicates that the scale bars (2 µm or 3 µm) were automatically generated by the SEM software (Zeiss NTS system) and represent the true magnification for each image.

3.6. Preliminary Cost Consideration

From an economic perspective, the use of WWFA aligns with the principles of the European Union's Circular Economy strategy, which prioritizes waste valorization and recycling over disposal. At present, WWFA is an industrial by-product with no commercial value, typically stored or landfilled. Therefore, WWFA waste is currently free of charge. It is expected that, with wider implementation of waste recycling policies, ash producers may even compensate end users for utilizing this residue. This work focuses on demonstrating the technical feasibility of WWFA valorization. A detailed cost analysis will be conducted in future studies once the process is optimized for pilot-scale production.

4. Conclusions

This study confirms the potential of utilizing WWFA and hydrated lime to produce ALWAs through cold-bonded granulation and carbonation curing. The granulation process proved effective in forming spherical aggregates, with performance influenced by material properties and granulator settings. All produced ALWAs satisfied the EN 13055:2016 classification criteria for lightweight aggregates, with bulk densities ranging from 1010.9 to 1060.0 kg/m^3 and particle densities between 1551.1 and 1584.8 kg/m^3. The WWFA-to-binder ratio significantly influenced granulation yield: the 0.28 ratio produced up to 2.5 times more 4/16 fraction compared to the 0.32 ratio, underlining its importance in determining aggregate production efficiency. Although the water absorption values

(23.5–25.1%) were slightly higher than those of LECAs (21.1%), they remained within acceptable limits for lightweight applications. Mechanical testing revealed that the A0.28 L formulation achieved the highest crushing resistance (2.74 N/mm^2), exceeding the performance of LECAs and demonstrating the structural viability of WWFA-based aggregates. XRD analysis confirmed calcite formation (CaCO$_3$) through carbonation, while XRF verified the presence of CaO in WWFA, which enhances additional carbonative activity. The measured pH levels (10.42–12.09) indicated suitable chemical stability. Freeze–thaw testing showed mass loss values between 5.50% and 9.46%, indicating moderate resistance and suitability for non-structural or moderately exposed applications. In addition, SEM analysis revealed microstructural differences among the aggregate formulations, depending on their composition. SEM analysis confirmed that binder content and carbonation strongly influenced ALWA microstructure. Low w/m mixtures (A0.32 L) produced compact, dense matrices, while higher w/m ratios (A0.30 L, A0.28 L) showed more porous, fragmented textures with voids and unreacted ash. Compared to LECAs, all ALWAs exhibited finer pore structures, demonstrating the effect of mixture design on porosity. At higher magnification, CaCO$_3$ was visible as dense deposits in A0.32 L, scattered crystals in A0.30 L, and needle-like precipitates in A0.28 L, confirming effective carbonation. These features explain the higher crushing resistance of ALWAs and highlight their potential as sustainable alternatives to conventional lightweight materials. The results of this study demonstrated that WWFA can be used to produce ALWAs through green technology based on carbonation with absorbed CO$_2$ gases. Furthermore, the low concentrations of chlorine and heavy metals in the WWFA were effectively stabilized during carbonation, suggesting that the produced aggregates are environmentally safe alternatives to LECAs for lightweight, non-structural applications.

References

1. Agrela, F.; Cabrera, M.; Morales, M.M.; Zamorano, M.; Alshaaer, M. Biomass fly ash and biomass bottom ash. In *New Trends in Eco-Efficient and Recycled Concrete*; Woodhead Publishing: Amsterdam, The Netherlands, 2019; pp. 23–58. Available online: https://www.sciencedirect.com/science/article/abs/pii/B9780081024805000026 (accessed on 8 September 2025).
2. Liang, X.; Li, Z.; Dong, H.; Ye, G. A review on the characteristics of wood biomass fly ash and their influences on the valorization in cementitious materials. *J. Build. Eng.* **2024**, *97*, 110927. [CrossRef]
3. Schlupp, F.; Page, J.; Djelal, C.; Libessart, L. Use of Biomass Bottom Ash as an Alternative Solution to Natural Aggregates in Concrete Applications: A Review. *Materials* **2024**, *17*, 4504. [CrossRef]
4. da Costa, T.P.; Quinteiro, P.; Arroja, L.; Dias, A.C. Environmental performance of different end-of-life alternatives of wood fly ash by a consequential perspective. *Sustain. Mater. Technol.* **2022**, *32*, e00411. [CrossRef]
5. Vaiciene, M.; Malaiskiene, J. The Impact of Wood Waste Ash on Physical Mechanical Properties of Concrete. *IOP Conf. Ser. Mater. Sci. Eng.* **2021**, *1203*, 032097. [CrossRef]
6. Siddique, R. Utilization of wood ash in concrete manufacturing. *Resour. Conserv. Recycl.* **2012**, *67*, 27–33. [CrossRef]

7.	Huotari, N.; Tillman-Sutela, E.; Moilanen, M.; Laiho, R. Recycling of ash—For the good of the environment? *For. Ecol. Manag.* **2015**, *348*, 226–240. [CrossRef]

8.	Ovčačíková, H.; Velička, M.; Vlček, J.; Topinková, M.; Klárová, M.; Burda, J. Corrosive Effect of Wood Ash Produced by Biomass Combustion on Refractory Materials in a Binary Al–Si System. *Materials* **2022**, *15*, 5796. [CrossRef] [PubMed]

9.	Odzijewicz, J.I.; Wołejko, E.; Wydro, U.; Wasil, M.; Jabłońska-Trypuć, A. Utilization of Ashes from Biomass Combustion. *Energies* **2022**, *15*, 9653. [CrossRef]

10.	Maj, I.; Niesporek, K.; Płaza, P.; Maier, J.; Łój, P. Biomass Ash: A Review of Chemical Compositions and Management Trends. *Sustainability* **2025**, *17*, 4925. [CrossRef]

11.	Teker Ercan, E.E.; Andreas, L.; Cwirzen, A.; Habermehl-Cwirzen, K. Wood Ash as Sustainable Alternative Raw Material for the Production of Concrete—A Review. *Materials* **2023**, *16*, 2557. [CrossRef]

12.	Options for Increased Use of Ash from Biomass Combustion and Co-Firing—Bioenergy. Available online: https://www.ieabioenergy.com/blog/publications/options-for-increased-use-of-ash-from-biomass-combustion-and-co-firing/ (accessed on 14 October 2025).

13.	*EN 13055:2016*; Lightweight Aggregates. European Committee for Standardization: Brussels, Belgium, 2016. Available online: https://standards.iteh.ai/catalog/standards/cen/a8e87cdf-860c-4bee-996e-822826ffa148/en-13055-2016 (accessed on 8 September 2025).

14.	Singh, N.; Raza, J.; Colangelo, F.; Farina, I. Advancements in Lightweight Artificial Aggregates: Typologies, Compositions, Applications, and Prospects for the Future. *Sustainability* **2024**, *16*, 9329. [CrossRef]

15.	Aggregates Analysis 2025 and Forecasts 2033: Unveiling Growth Opportunities. Available online: https://www.promarketreports.com/reports/aggregates-71869 (accessed on 8 September 2025).

16.	Ogundana, A.K.; Afolalu, S.A. Environmental and Social Implications of Aggregate Extraction: A Review. In Proceedings of the International Conference on Science, Engineering and Business for Driving Sustainable Development Goals (SEB4SDG), Omu-Aran, Nigeria, 2–4 April 2024.

17.	Properties of Lightweight Aggregates Made with Cold Bonded Pelletization of Fly Ash, Metakaolin, and Cement. Available online: https://www.researchgate.net/publication/266323726_Properties_of_Lightweight_Aggregates_Made_with_Cold_Bonded_Pelletization_of_Fly_Ash_Metakaolin_and_Cement (accessed on 8 September 2025).

18.	Recycling and Disposal of Wood Ash. Fire Research and Management Exchange System. Available online: https://www.frames.gov/catalog/35093 (accessed on 8 September 2025).

19.	Demeyer, A.; Voundi Nkana, J.C.; Verloo, M.G. Characteristics of wood ash and influence on soil properties and nutrient uptake: An overview. *Bioresour. Technol.* **2001**, *77*, 287–295. [CrossRef] [PubMed]

20.	Yin, C.; Rosendahl, L.A.; Kær, S.K. Grate-firing of biomass for heat and power production. *Prog. Energy Combust. Sci.* **2008**, *34*, 725–754. [CrossRef]

21.	AL-Kharabsheh, B.N.; Arbili, M.M.; Majdi, A.; Ahmad, J.; Deifalla, A.F.; Hakamy, A. A Review on Strength and Durability Properties of Wooden Ash Based Concrete. *Materials* **2022**, *15*, 7282. [CrossRef]

22.	Kursula, K.; Perumal, P.; Ohenoja, K.; Illikainen, M. Production of artificial aggregates by granulation and carbonation of recycled concrete fines. *J. Mater. Cycles Waste Manag.* **2022**, *24*, 2141–2150. [CrossRef]

23.	Tesovnik, A.; Ottosen, L.M.; Ducman, V. Carbonation of lightweight alkali-activated aggregates based on biomass fly ash: Effect on microstructure and leaching behavior. *Case Stud. Constr. Mater.* **2025**, *23*, e05014. [CrossRef]

24.	Ma, J.; Dai, G.; Jiang, F.; Wang, N.; Zhao, Y.; Wang, X. Effect of Carbonation Treatment on the Properties of Steel Slag Aggregate. *Materials* **2023**, *16*, 5768. [CrossRef]

25.	Chi, J.M.; Huang, R.; Yang, C.C.; Chang, J.J. Effect of aggregate properties on the strength and stiffness of lightweight concrete. *Cem. Concr. Compos.* **2003**, *25*, 197–205. [CrossRef]

26.	Lin, J.; Tan, T.H.; Yeo, J.S.; Goh, Y.; Ling, T.C.; Mo, K.H. Municipal woody biomass waste ash-based cold-bonded artificial lightweight aggregate produced by one-part alkali-activation method. *Constr. Build Mater.* **2023**, *394*, 131619. [CrossRef]

27.	*EN 933-1:2012*; Tests for Geometrical Properties of Aggregates—Part 1: Determination of Particle. European Committee for Standardization: Brussels, Belgium, 2012. Available online: https://standards.iteh.ai/catalog/standards/cen/100b983f-85a4-4a80-934c-e93c584dbdb4/en-933-1-2012?srsltid=AfmBOopgJUgLSn6ZX7oQCYSNROZGKwSbX_Xrp7Qhy_9eokVWQzbC-P0D (accessed on 20 October 2025).

28.	*EN 1097-11:2013*; Tests for Mechanical and Physical Properties of Aggregates—Part 11: [Internet]. European Committee for Standardization: Brussels, Belgium, 2013. Available online: https://standards.iteh.ai/catalog/standards/cen/965c5da7-1e34-413e-91f3-92e66b008323/en-1097-11-2013?srsltid=AfmBOopjjeQr2CPb-_-k0i4kQZ5lZsMmFuSYL7stj8Yi0fcrlSsP0jDM (accessed on 13 October 2025).

29. *EN 1097-2:2020*; Tests for Mechanical and Physical Properties of Aggregates—Part 2: Methods for [Internet]. European Committee for Standardization: Brussels, Belgium, 2020. Available online: https://standards.iteh.ai/catalog/standards/cen/2b59008c-ab4d-428f-9e85-780705498a57/en-1097-2-2020?srsltid=AfmBOoqk57MGW4uqsp2sRCb0Ufd_BbmGJpcd0-YcCWT-0kwZ5ojPscb1 (accessed on 13 October 2025).

30. *EN 1097-3:1998*; Tests for Mechanical and Physical Properties of Aggregates—Part 3: Determination. European Committee for Standardization: Brussels, Belgium, 1998. Available online: https://standards.iteh.ai/catalog/standards/cen/1e043df4-6c8e-423c-9ba7-3bcb715a6cf3/en-1097-3-1998?srsltid=AfmBOoqcfKwdh3nFU17wXSOc-56CzuH94hPm-JtFOdvQvFopcj3U0eoR (accessed on 13 October 2025).

31. *EN 1097-6:2022*; Tests for Mechanical and Physical Properties of Aggregates—Part 6: Determination. European Committee for Standardization: Brussels, Belgium, 2022. Available online: https://standards.iteh.ai/catalog/standards/cen/7eb55eec-cf2d-449c-bdf5-45534b169181/en-1097-6-2022 (accessed on 15 September 2025).

32. *EN 1367-7:2014*; Tests for Thermal and Weathering Properties of Aggregates—Part 7: Determination. European Committee for Standardization: Brussels, Belgium, 2014. Available online: https://standards.iteh.ai/catalog/standards/cen/c8a31143-2286-4a16-b988-dda6fca2c0e9/en-1367-7-2014?srsltid=AfmBOopiKF3k5HerU9Rtkho1E1p5xBh0wO5NhVYQI2D3zpqnuWZha94n (accessed on 15 September 2025).

33. Dong, B.; Chen, C.; Wei, G.; Fang, G.; Wu, K.; Wang, Y. Fly ash-based artificial aggregates synthesized through alkali-activated cold-bonded pelletization technology. *Constr. Build. Mater.* **2022**, *344*, 128268. [CrossRef]

34. Shen, Z.; Zhu, H.; Meng, X.C. The influence of curing methods on the performance of recycled concrete powder artificial aggregates and concrete. *Constr. Build. Mater.* **2024**, *435*, 136908. [CrossRef]

35. Liang, X.; Dong, H.; Li, Z.; Liu, C.; Zhang, S.; Ye, G. Characterization, pretreatment, and valorization of wood biomass fly ash in a binary cement-free binder. *Dev. Built Environ.* **2025**, *23*, 100700. [CrossRef]

36. Martínez-García, R.; Jagadesh, P.; Zaid, O.; Șerbănoiu, A.A.; Fraile-Fernández, F.J.; de Prado-Gil, J.; Qaidi, S.M.A.; Grădinaru, C.M. The Present State of the Use of Waste Wood Ash as an Eco-Efficient Construction Material: A Review. *Materials* **2022**, *15*, 5349. [CrossRef] [PubMed]

37. Ndahirwa, D.; Zmamou, H.; Lenormand, H.; Chenot, E.; Potel, S.; Leblanc, N. Wood ash-based binders for lightweight building materials: Evaluating the influence of hydraulic lime and cement on the setting and mechanical properties of wood ash pastes. *Results Eng.* **2024**, *24*, 102738. [CrossRef]

38. Viola, V.; Catauro, M.; D'Amore, A.; Perumal, P. Assessing the carbonation potential of wood ash for CO_2 sequestration. *Low-Carbon Mater. Green Constr.* **2024**, *2*, 12. [CrossRef]

39. Tripathi, N.; Hills, C.D.; Singh, R.S.; Kyeremeh, S.; Hurt, A. Mineralisation of CO_2 in wood biomass ash for cement substitution in construction products. *Front. Sustain.* **2024**, *5*, 1287543. [CrossRef]

40. Morandeau, A.; Thiéry, M.; Dangla, P. Investigation of the carbonation mechanism of CH and C-S-H in terms of kinetics, microstructure changes and moisture properties. *Cem. Concr. Res.* **2014**, *56*, 153–170. [CrossRef]